Aerospace Science and Technology 33 (2014) 107–117

Contents lists available at ScienceDirect

Aerospace Science and Technology

www.elsevier.com/locate/aescte

# Extended state observer based robust control of wing rock motion

Deepak Kumar Kori [a,1], Jaywant P. Kolhe [b,2], S.E. Talole [a,*,3]

[a] Department of Aerospace Engineering, Defence Institute of Advanced Technology, Girinagar, Pune 411025, India
[b] Research and Development Estt. (Engrs), Dighi, Pune 411015, India

ARTICLE INFO

*Article history:*
Received 18 October 2013
Received in revised form 14 January 2014
Accepted 20 January 2014
Available online 27 January 2014

*Keywords:*
Wing rock motion
Robust control
Extended state observer

ABSTRACT

In this paper, a new design based on the Extended State Observer (ESO) technique for the robust control of wing rock motion of slender delta wings is proposed. The wing rock motion dynamics with varying angle of attack is significantly uncertain. The ESO is employed to simultaneously estimate the state and the uncertainty. The estimated uncertainty is used to robustify an Input–Output Linearization based controller designed for the nominal system. Closed loop stability of the overall system is established. The notable feature of the proposed design is that it neither requires accurate plant model nor any information about the uncertainty. The effectiveness of the ESO in estimation of the uncertainties and states and in regulating the rolling motion in the presence of significant uncertainties and un-modeled servo and sideslip dynamics is illustrated by simulation. Lastly, the efficacy of the proposed design is demonstrated by comparing its performance with some well-known existing designs.



## 1. Introduction

Wing rock motion is a concern for combat aircraft because it may have adverse effects on maneuverability, tracking accuracy, and operational safety. Unsteady aerodynamic effects at high angle of attack generate wing rock phenomenon in case of slender delta wing aircraft and is a complicated aerodynamic phenomenon, characterized by self-induced limit-cycle roll oscillations. The maneuvering envelope of an aircraft exhibiting this behavior gets seriously restricted because the maximum incidence angle is often limited by the onset of wing rock before the occurrence of stall [25]. Since high performance aircraft have mission requirements for operating at high angles of attack, the control of wing rock motion is of significant importance.

The wing rock motion needs to be controlled as it causes maneuver limitation ranging in severity from degradation in tracking effectiveness to loss of control. There are three possible approaches to suppress or prevent wing rock [1] such as reshaping the airframe configuration, by adopting maneuver limiting and by employing stability augmentation or automatic flight control system of which the last one has become the most effective method for attaining strong resistance to wing rock without degrading maneuverability. However, as the dynamics of the wing rock phenomenon change nonlinearly with the angle of attack, the problem of designing controllers that are robust against changes in angle of attack coupled with presence of system uncertainties and external disturbances pose a great challenge. In literature one can find application of various theories towards designing controllers for regulating the wing rock motion. Formulations based on nonlinear $H_\infty$ approach [25], feedback linearization [20], adaptive control [3,27], optimal control [1,19,26], variable phase control [17], sliding-mode fuzzy neural network based design [18], variable structure model reference adaptive control [2], and design based on uncertainty and disturbance estimation technique [35] are some examples to mention.

In general in the designs appeared in literature, some issues need attention. Owing to the complex nonlinear behavior of the wing rock phenomenon and its dependence on the angle of attack, usually the controllers have been designed by considering a fixed angle of attack. In some cases, the controllers are tested at other angles of attack to prove robustness of the designs. Requirement of availability of an accurate mathematical model for designing controller is another concern. For example, the designs based on feedback linearization need accurate mathematical model, a requirement which is hard to meet in practice. In some approaches, such as the designs based on variable structure control or Lyapunov theory, usually the knowledge of bound on uncertainty and disturbances is necessary for successful design of the controller. Lastly, the issue related to tackling external disturbances is often ignored in the designs.

In this work, an Extended State Observer (ESO) based robust control design is proposed for suppressing the wing rock motion with time-varying angle of attack. To address the issues of uncertainties and external disturbances, an ESO is designed and integrated with the Input–Output Linearization (IOL) controller to

* Corresponding author.
*E-mail address:* setalole@hotmail.com (S.E. Talole).
[1] Postgraduate student.
[2] Scientist.
[3] Professor.

1270-9638/$ – see front matter 
http://dx.doi.org/10.1016/j.ast.2014.01.008

achieve robustness. The design is relatively less dependent on the availability of accurate mathematical model and also does not need any information such as bound or any other characterization of the uncertainties and disturbances. The resulting design essentially follows the principle of the well-known Active Disturbance Rejection Control (ADRC) technique. The basic idea in ADRC is to estimate the effect of unknown plant dynamics, uncertainties and disturbances using an ESO and to actively compensate for the same in the control law in real-time. In general, the ADRC approach [9,13,31] consists of tracking differentiator also referred to as profile generator or reference generator, an ESO and a PD controller. Although originally, the components of ADRC were presented in the nonlinear set up, i.e., nonlinear tracking differentiator, nonlinear ESO and nonlinear PD control, extension of the ADRC with linear ESO and PD control [40] designated as LARDC have also been widely studied and reported in the literature. The work presented here employs Input–Output Linearization (IOL) approach for designing the wing rock motion controller. The IOL control has been robustified by using the ESO. The resulting controller design, in essence, results into ADRC employing ESO and PD control and therefore, follows the principle of ADRC in linear set-up. Numerical simulations are carried out and the results are presented to demonstrate efficacy of the design.

## 2. Wing rock dynamics

Owing to its highly nonlinear characteristics, various approaches have been presented to model the wing rock phenomena [6,11,14,22,23]. In [23], the models presented in [6] and [22] are used with varying angle of attack scenario and the authors have proposed an interpolation function which interpolates smoothly the aerodynamic coefficients with corresponding angles of attack. Further, it is shown that the interpolated values are in close proximity to the coefficients at different angles of attacks as given in [22]. In this work, the model presented in [23] is used for designing an ESO based robust controller for suppression of wing rock motion. To this end, the equations governing the wing rock dynamics are given by

$$\begin{aligned}\ddot{\phi} &= -\omega_j^2\phi + \mu_1^j\dot{\phi} + b_1^j\dot{\phi}^3 + \mu_2^j\phi^2\dot{\phi} + b_2^j\phi\dot{\phi}^2 + g\delta\\ y &= \phi\end{aligned} \tag{1}$$

where $\phi$, $\delta$, and $g$ represent the roll angle, aileron deflection and input gain respectively, $\omega_j^2$, $\mu_1^j$, $\mu_2^j$, $b_1^j$, $b_2^j$ are the values of aerodynamic coefficients at angle of attack $\alpha_j$. Relations for the system coefficients appearing in (1) are

$$\begin{aligned}\omega_j^2 &= -c_1a_1^j\\ \mu_1^j &= c_1a_2^j - c_2\\ b_1^j &= c_1a_3^j\\ \mu_2^j &= c_1a_4^j\\ b_2^j &= c_1a_5^j\end{aligned} \tag{2}$$

where the coefficients depend on the parameters $a_i^j$, which in turn are functions of the angle of attack $\alpha$. The values of the parameters $a_i^j$ for various angles of attack are given in Table 1. In order to build a smooth, time-varying model of the wing rock that depends on angle of attack, the following interpolation function has been proposed

$$\rho_j(\alpha) = \frac{e^{-(\frac{\alpha-\alpha_j}{s_j})^2}}{\sum_{l=1}^{7} e^{-(\frac{\alpha-\alpha_l}{s_l})^2}} \tag{3}$$

where the centers $\alpha_j$ and spreads $s_j$ are as given in Table 2.

**Table 1**
Parameters for the coefficients in the wing rock model.

| $\alpha$ | $a_1^j$ | $a_2^j$ | $a_3^j$ | $a_4^j$ | $a_5^j$ |
|---|---|---|---|---|---|
| 15 | −0.01026 | −0.02117 | −0.14181 | 0.99735 | −0.83478 |
| 17 | −0.02007 | −0.0102 | −0.0837 | 0.63333 | −0.5034 |
| 19 | −0.0298 | 0.000818 | −0.0255 | 0.2692 | −0.1719 |
| 21.5 | −0.04207 | 0.01456 | 0.04714 | −0.18583 | 0.24234 |
| 22.5 | −0.04681 | 0.01966 | 0.05671 | −0.22691 | 0.59065 |
| 23.75 | −0.0518 | 0.0261 | 0.065 | −0.2933 | 1.0294 |
| 25 | −0.05686 | 0.03254 | 0.07334 | −0.3597 | 1.4681 |

**Table 2**
Centers and spreads for wing rock interpolation.

| $j$ | 1 | 2 | 3 | 4 | 5 | 6 | 7 |
|---|---|---|---|---|---|---|---|
| $\alpha_j$ | 15 | 17 | 19 | 21.5 | 22.5 | 23.75 | 25 |
| $s_j$ | 1.5 | 1.5 | 1.5 | 2.0 | 1 | 1 | 1 |

With $x_1 = \phi$, $x_2 = \dot{\phi}$ the time-varying wing rock model can be written in state space form as

$$\begin{aligned}\dot{x}_1 &= x_2\\ \dot{x}_2 &= \sum_{j=1}^{7}\rho_j(\alpha)\left(-\omega_j^2x_1 + \mu_1^jx_2 + b_1^jx_2^3 + \mu_2^jx_1^2x_2 + b_2^jx_1x_2^2\right) + g\delta\\ y &= x_1\end{aligned} \tag{4}$$

It is assumed that the angle of attack, $\alpha$, varies according to an exogenous dynamical system

$$\begin{bmatrix}\dot{\alpha}_1\\ \dot{\alpha}_2\end{bmatrix} = \begin{bmatrix}0 & 25\\ -25 & -10\end{bmatrix}\begin{bmatrix}\alpha_1\\ \alpha_2\end{bmatrix} + \begin{bmatrix}0\\ 500\end{bmatrix} + \begin{bmatrix}0\\ 62.5\end{bmatrix}r \tag{5}$$

where $\alpha_1 = \alpha$ and $r$ is the command input that can take values between $-1$ and $+1$. This system has been chosen without a basis on physical aircraft dynamics, but it could represent the effects of the aircraft itself which receives the pilot's commands through the input $r$.

In [22], the authors have analyzed that the wing rock model has a stable focus at the origin for the angle of attack $\alpha$ less than 19.5°. For higher angles, the origin becomes an unstable equilibrium and limit cycle behavior is observed. For example, simulations results for an angle of attack of 21.5 degrees with initial conditions of $\phi(0) = 20$ deg and $p(0) = 0$ deg/s are given in Fig. 1 from where it can be observed that the roll angle history exhibits oscillatory motion and the limit cycle behavior. In the present work, it is considered that the angle of attack varies between 15 to 25° so that the qualitative behavior of (4) changes periodically as $\alpha$ becomes smaller or larger than 19.5°. The control objective is to design a robust controller using only roll angle feedback such that the wing rock motion is suppressed and the roll angle is regulated to zero confirming the imposed specifications.

## 3. Extended state observer

As real plants are usually affected by significant uncertainties and unmeasurable external disturbances, disturbance rejection or compensation has become an important problem for high performance control system design. A great deal of effort has been devoted to address this issue and consequently number of methods/approaches have been proposed to robustify systems in presence of the uncertainties and disturbances [4,12,21,32,41].

One well-known approach that can be used in designing robust control systems is the Extended State Observer (ESO) [8,37,40,44]. The ESO can estimate the uncertainties along with the states of the system enabling disturbance rejection or compensation. In [37], a comparison study of the performances and characteristics of

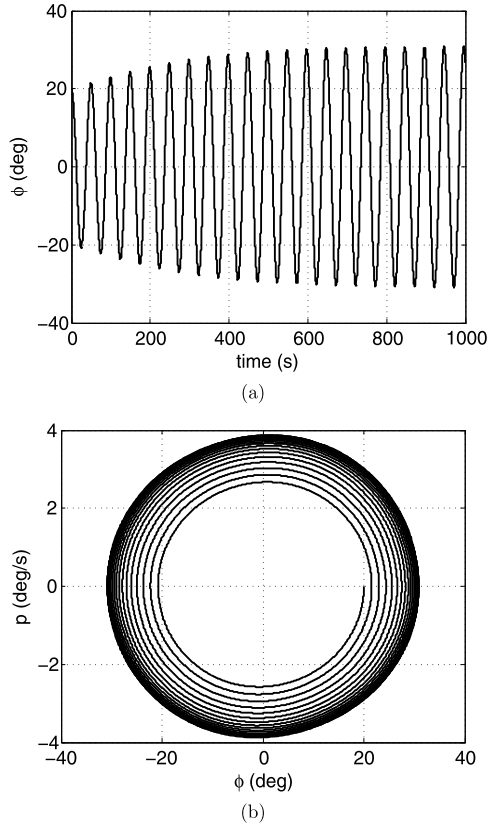


**Fig. 1.** Wing rock motion: (a) roll angle and (b) limit cycle.

three advanced state observers namely high gain observer, ESO and Sliding Mode Observer are presented and the authors have shown that overall the ESO is superior in dealing with the uncertainties, disturbances and sensor noise. A large number of applications of ESO based control strategies in diverse fields have appeared in the literature [7,24,29,30,33,34,38,39,42,43].

In this section a brief review of this approach is presented for the sake of completeness and the reader may refer to various cited references for more details.

### 3.1. Concept of ESO

Consider a second order nonlinear system described by

$$\ddot{y} = f(y, \dot{y}, w) + b_o u \tag{6}$$

where $f(.)$ represents dynamics of the plant and the disturbance and is assumed to be unknown, $w$ is the unknown input disturbance, $u$ is the control signal, and $y$ is the measured output. The quantity $b_o$ is assumed to be known and $f(.)$ is usually a nonlinear function. The plant (6) is first augmented as

$$\begin{aligned} \dot{x}_1 &= x_2 \\ \dot{x}_2 &= x_3 + b_o u \\ \dot{x}_3 &= h \\ y &= x_1 \end{aligned} \tag{7}$$

where $f(y, \dot{y}, w)$ is treated as an extended state $x_3$, i.e., $x_3 = f(y, \dot{y}, w)$. Here $h = \dot{f}(.)$ is assumed to be unknown but bounded function. By making $f(.)$ a state, however, it is now possible to estimate it by using a state estimator. To this end, consider a nonlinear observer for the system (7) as

$$\begin{aligned} \dot{\hat{x}}_1 &= \hat{x}_2 + \beta_1 g_1(e_{o1}) \\ \dot{\hat{x}}_2 &= \hat{x}_3 + \beta_2 g_2(e_{o1}) + b_o u \\ \dot{\hat{x}}_3 &= \beta_3 g_3(e_{o1}) \end{aligned} \tag{8}$$

where $e_{o_1} = y - \hat{x}_1 = x_1 - \hat{x}_1$ and $\hat{x}_3$ is an estimate of the uncertainty. The terms $\beta_i$ are the observer gains and $g_i(.)$ are a set of suitably constructed nonlinear gain functions satisfying $e_{o_1} g_i(e_{o_1}) > 0$, $\forall e_{o_1} \neq 0$ and $g_i(0) = 0$. If the nonlinear functions, $g_i(.)$, and their related parameters are chosen properly, the estimated state variables $\hat{x}_i$ are expected to converge to the respective states of the system $x_i$, i.e., $\hat{x}_i \to x_i$; $i = 1, 2, 3$.

The choice of the nonlinear function is an important aspect in the ESO design. The general expression for these functions, selected heuristically based on experimental results is

$$g_i(e_{o_1}, \kappa_i, \epsilon) = \begin{cases} |e_{o_1}|^{\kappa_i} \operatorname{sign}(e_{o_1}), & |e_{o_1}| > \epsilon \\ \frac{e_{o_1}}{\epsilon^{1-\kappa_i}}, & |e_{o_1}| \leqslant \epsilon \end{cases} \quad i = 1, 2, 3 \tag{9}$$

where $\epsilon > 0$. An important feature of these functions is that for $0 < \kappa_i < 1$, $g_i(.)$ yields relatively high gain when error is small and small gain when the error is large. The constant $\epsilon$ is a small number used to limit the gain in the neighborhood of the origin and defines the range of the error corresponding to high gain.

### 3.2. Linear ESO

The ESO of (8) with the gains given in (9) is called as the nonlinear ESO or NESO as it employs the nonlinear gain functions. On the other hand if one chooses $g_i(e_{o_1}) = e_{o_1}$, the ESO takes the form of the conventional Luenberger observer and is designated as linear ESO or LESO. It can be noted that the LESO essentially represents a special case of the nonlinear ESO if one chooses the NESO parameters, $\kappa_i$'s, as unity. Now writing the extended order system (7) in state space notation as

$$\dot{x} = Ax + Bu + Eh \tag{10}$$

where $x = [x_1 \ x_2 \ x_3]^T$ is the state vector of the extended order system and

$$A = \begin{bmatrix} 0 & 1 & 0 \\ 0 & 0 & 1 \\ 0 & 0 & 0 \end{bmatrix}, \qquad B = \begin{bmatrix} 0 \\ b_o \\ 0 \end{bmatrix}, \qquad E = \begin{bmatrix} 0 \\ 0 \\ 1 \end{bmatrix}$$

and $C = [1 \ 0 \ 0]$. The LESO for the system (10) is given by (8) with the gains $g(e_{o_1}) = e_{o_1}$. The state space model of the LESO dynamics can be written as

$$\dot{\hat{x}} = A\hat{x} + Bu + LC(x - \hat{x}) \tag{11}$$

where

$$L = [\beta_1 \ \ \beta_2 \ \ \beta_3]^T \tag{12}$$

is the observer gain vector. In the present work, the LESO is employed instead of the NESO as the use of linear ESO offers certain advantages. Firstly, the observer gains can be chosen systematically through pole placement whereas the various parameters appearing in NESO are usually chosen by trial and error procedure. Secondly the closed loop stability for LESO can be established conclusively as shown in the next section. Lastly, the LESO is easy from hardware implementation point of view.

### 3.3. ESO based controller

In this work, the ESO is employed for designing a robust controller for wing rock motion control. To this end, consider the dynamics given by (4). Since in practice system model is rarely

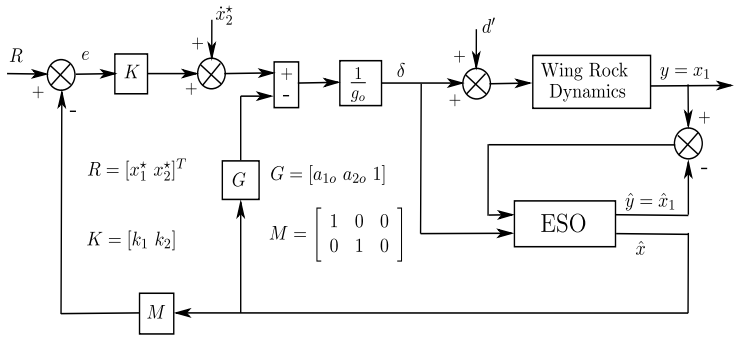


**Fig. 2.** Functional block diagram of the ESO-based controller.

known exactly, it becomes necessary to account for the modeling errors and inaccuracies. To this end, the input gain, $g$, is taken as $g = g_o + \Delta g$ where $g_o$ represents the nominal value of $g$ whereas $\Delta g$ is its associated uncertainty. To account for uncertainties, system nonlinearities and external disturbances, the dynamics of (4) is re-written as

$$\ddot{y} = \left[a_o \bar{y} + (a - a_o \bar{y}) + (g - g_o)\delta\right] + g_o \delta + d' \tag{13}$$

where $a_o = [-\omega_{jo}^2 \; \mu_{1o}^j]$, $\bar{y} = [\phi \; \dot{\phi}]^T$, and $a = \sum_{j=1}^{7} \rho_j(\alpha)(-\omega_j^2 \phi + \mu_1^j \dot{\phi} + b_1^j \dot{\phi}^3 + \mu_2^j \phi^2 \dot{\phi} + b_2^j \phi \dot{\phi}^2)$. In essence, the term $a_o \bar{y}$ contains terms that are linear in output, $y$, and its derivative. The quantity, $d'$, represents the effect of external disturbances, if any. Note here that $\omega_{jo}^2$ and $\mu_{1o}^j$ are the nominal values of $\omega_j^2$ and $\mu_1^j$ respectively. Now defining the total uncertainty, $d$, as

$$d = (a - a_o \bar{y}) + (g - g_o)\delta + d' \tag{14}$$

the dynamics of (13) takes the form

$$\ddot{y} = a_o \bar{y} + g_o \delta + d \tag{15}$$

Now defining $x_1 = y$ and $x_2 = \dot{y}$, the dynamics of (15) can be re-written in a phase variable state space model form as

$$\begin{aligned} \dot{x}_1 &= x_2 \\ \dot{x}_2 &= a_{1o} x_1 + a_{2o} x_2 + g_o \delta + d \\ y &= x_1 \end{aligned} \tag{16}$$

where, $a_{1o} = -\omega_{jo}^2$ and $a_{2o} = \mu_{1o}^j$. Re-writing (16) compactly as

$$\begin{aligned} \dot{x}_p &= A_p x_p + B_p \delta + B_d d \\ y_p &= C_p x_p \end{aligned} \tag{17}$$

where $x_p = [x_1 \; x_2]^T = [y \; \dot{y}]^T$ is the state vector and

$$A_p = \begin{bmatrix} 0 & 1 \\ a_{1o} & a_{2o} \end{bmatrix}, \qquad B_p = \begin{bmatrix} 0 \\ g_o \end{bmatrix}$$

$$B_d = \begin{bmatrix} 0 \\ 1 \end{bmatrix}, \qquad C_p = [1 \quad 0]$$

Following the Input–Output Linearization approach [28], the control that would achieve the roll angle regulation is designed as

$$\delta = \frac{1}{g_o}(-a_{1o} x_1 - a_{2o} x_2 - k_2 x_2 - k_1 x_1 - d) \tag{18}$$

where $k_i$s are the controller gains which need to be chosen so as to satisfy the desired performance specifications. However, to implement the control law (18) one needs knowledge of the uncertainty, $d$, apart from the state variables. Here, the same are estimated by employing the Extended State Observer. To this end, defining $x_3 = d$, the extended order system for the plant (17) is obtained as

$$\dot{x} = Ax + B\delta + Eh \tag{19}$$

where $x = [x_1 \; x_2 \; x_3]^T$ is the state vector of the extended order system and

$$A = \begin{bmatrix} 0 & 1 & 0 \\ a_{1o} & a_{2o} & 1 \\ 0 & 0 & 0 \end{bmatrix}, \qquad B = \begin{bmatrix} 0 \\ g_o \\ 0 \end{bmatrix}, \qquad E = \begin{bmatrix} 0 \\ 0 \\ 1 \end{bmatrix}$$

To obtain estimate of the state and uncertainty, a linear ESO of the form (11) can be designed as follows,

$$\dot{\hat{x}} = A\hat{x} + B\delta + LC(x - \hat{x}) \tag{20}$$

where $C = [1 \; 0 \; 0]$ and $L = [\beta_1 \; \beta_2 \; \beta_3]^T$ is the observer gain vector. Using the estimate in (18), the resulting controller takes the form as

$$\delta = \frac{1}{g_o}(-a_{1o}\hat{x}_1 - a_{2o}\hat{x}_2 - k_2\hat{x}_2 - k_1\hat{x}_1 - \hat{x}_3) \tag{21}$$

where $\hat{x}_3$ is the estimate of the uncertainty, $d$. Having the estimate of the state $x_2$ and the uncertainty, the controller (21) is implementable and is designated as the ESO based controller. A functional block diagram of the ESO based controller is shown in Fig. 2 wherein for roll regulation, the reference quantities are to be taken as zero.

## 4. Closed loop stability

In this section, results on closed stability [14,33] are presented. To this end, consider the state equation of (17)

$$\dot{x}_p = A_p x_p + B_p \delta + B_d d \tag{22}$$

The controller (21) can be re-written as

$$\delta = -K_p \hat{x}_p - \frac{1}{g_o}\hat{x}_3 \tag{23}$$

where $K_p = \frac{1}{g_o}[(a_{1o} + k_1) \; (a_{2o} + k_2)]$ is the state feedback gain vector for the system (17) and $\hat{x}_p$ is the estimate of $x_p$. Using (22), (23), and carrying out some simplifications leads to the following tracking error dynamics

$$\dot{x}_p = (A_p - B_p K_p)x_p - [B_p K_p \; B_d]e_o \tag{24}$$

where $e_o$ is the observer estimation error vector, i.e., $e_o = x - \hat{x}$. Next, the observer error dynamics is obtained by subtracting (20) from (19) as

$$\dot{e}_o = (A - LC)e_o + Eh \tag{25}$$

Combining (24) and (25) yields

$$\begin{bmatrix}\dot{x}_p\\ \dot{e}_o\end{bmatrix}=\begin{bmatrix}(A_p-B_pK_p) & -[B_pK_p\ B_d]\\ 0 & (A-LC)\end{bmatrix}\begin{bmatrix}x_p\\ e_o\end{bmatrix}+\begin{bmatrix}0\\ E\end{bmatrix}h \tag{26}$$

For stability analysis results, the following assumptions are made [16]:

**Assumption 1.** The nonlinear function $(a-a_o\bar{y})$ in (13) where $\bar{y}=x_p=[\phi\ \dot{\phi}]^T$ is bounded for $\|x_p\|_2\leqslant B_{x_p}$, where $B_{x_p}$ is a constant.

**Assumption 2.** The rate of change of disturbance, i.e., $\dot{d}=h$ is bounded.

Under these assumptions, the results on observer error dynamics and closed loop system stability are presented as follows.

### 4.1. Observer error dynamics

**Theorem 1.** *Consider the observer error dynamics of (25). Under the Assumptions 1 and 2, if observer gain vector $L$ is chosen such that $(A-LC)$ is Hurwitz, then $e_o$ exponentially converges to the bounded ball $B_{r_1}=\{e_o\in\Re^3\mid\|e_o\|_2\leqslant 2\lambda_{\max}(P_o)h_{\max}\}$, where $(A-LC)^TP_o+P_o(A-LC)=-I$, $\lambda_{\max}(P_o)$ is the maximum eigenvalue of $P_o$ and $h_{\max}$ is the absolute maximum value of $h$.*

**Proof.** Define the Lyapunov function $V_o$ as

$$V_o=e_o^TP_oe_o \tag{27}$$

The derivative of $V_o$ with respect to time is

$$\begin{aligned}\dot{V}_o&=e_o^T\big[(A-LC)^TP_o+P_o(A-LC)\big]e_o+2e_o^TP_oEh\\&\leqslant-\|e_o\|_2^2+2h_{\max}\|P_o\|_2\|e_o\|_2\\&\leqslant-\|e_o\|_2\big(\|e_o\|_2-2\lambda_{\max}(P_o)h_{\max}\big)\end{aligned} \tag{28}$$

Thus $e_o$ exponentially converges to the bounded ball $B_{r_1}=\{e_o\in\Re^3\mid\|e_o\|_2\leqslant 2\lambda_{\max}(P_o)h_{\max}\}$. □

### 4.2. Closed loop stability

Next consider the closed loop dynamics given by (26). Defining $x_{cl}=[x_p\ e_o]^T$, closed loop dynamics of (26) can be re-written as

$$\dot{x}_{cl}=A_{cl}x_{cl}+B_{cl}h \tag{29}$$

where

$$A_{cl}=\begin{bmatrix}(A_p-B_pK_p) & -[B_pK_p\ B_d]\\ 0 & (A-LC)\end{bmatrix},\qquad B_{cl}=\begin{bmatrix}0\\ E\end{bmatrix}$$

**Theorem 2.** *Consider the closed loop system dynamics of (29). Under the Assumptions 1 and 2, if the gain vector $K_p$ and the observer gain vector $L$ are chosen such that $A_{cl}$ is Hurwitz, then $x_{cl}$ exponentially converges to the bounded ball $B_{r_2}=\{x_{cl}\in\Re^5\mid\|x_{cl}\|_2\leqslant 2\lambda_{\max}(P_{cl})h_{\max}\}$, where $A_{cl}^TP_{cl}+P_{cl}A_{cl}=-I$, $\lambda_{\max}(P_{cl})$ is the maximum eigenvalue of $P_{cl}$ and $h_{\max}$ is the absolute maximum value of $h$.*

**Proof.** Define the Lyapunov function $V_{cl}$ as

$$V_{cl}=x_{cl}^TP_{cl}x_{cl} \tag{30}$$

The derivative of $V_{cl}$ with respect to time is

$$\begin{aligned}\dot{V}_{cl}&=x_{cl}^T\big[A_{cl}^TP_{cl}+P_{cl}A_{cl}\big]x_{cl}+2x_{cl}^TP_{cl}B_{cl}h\\&\leqslant-\|x_{cl}\|_2^2+2h_{\max}\|P_{cl}\|_2\|x_{cl}\|_2\\&\leqslant-\|x_{cl}\|_2\big(\|x_{cl}\|_2-2\lambda_{\max}(P_{cl})h_{\max}\big)\end{aligned} \tag{31}$$

Thus $x_{cl}$ exponentially converges to the bounded ball $B_{r_2}=\{x_{cl}\in\Re^5\mid\|x_{cl}\|_2\leqslant 2\lambda_{\max}(P_{cl})h_{\max}\}$. □

From (26), it can be seen that the eigenvalues of the system matrix of the error dynamics are given by the eigenvalues of $(A_p-B_pK_p)$ and $(A-LC)$. Since the pair $(A_p,B_p)$ is controllable and the pair $(A,C)$ is observable, stability of the error dynamics (26) can always be ensured by placing the controller and observer poles appropriately. Further, since (26) is stable, it is obvious that under the assumption of boundedness of $h$, the bounded input-bounded output stability for the linear system (26) is assured. A special case arises when $h=0$, i.e., when the rate of change of uncertainty, $d$, is zero. In this case, the error dynamics (26) is asymptotically stable.

At this juncture, some comments on the performance of the ESO for non-constant disturbances are in order. From (25), it can be observed that the LESO offers asymptotic convergence of state estimate for constant disturbance case, i.e., for the case when rate of change of uncertainty is zero. One approach to achieve asymptotic convergence for LESO error dynamics for the class of disturbances that are time-varying but can be expressed in time polynomial function form such as $d(t)=d_0+d_1t+d_2t^2+\cdots$ is to use the generalized or higher order ESO [10]. With the generalized ESO, it can be shown that if the $r$th order derivative of disturbance is zero, then by designing an $r$th order ESO, i.e., by considering $r$ extended states, asymptotic convergence for the LESO state estimate can be achieved. Thus, asymptotic convergence for the commonly considered disturbances such as step, ramp and parabolic cases can be obtained using the ESO of 1st, 2nd, and 3rd order respectively. For the case of time varying disturbances, the higher order ESO has been shown to improve the estimation accuracy. For example in [10], performance analysis of higher order or generalized extended state observer (ESO) in handling fast-varying disturbances such as sinusoidal is presented and it is shown that the higher order ESO offers improvement in the estimation of fast-varying sinusoidal disturbances, if the ESO bandwidth is chosen sufficiently larger than the frequency of the disturbance. The authors have presented frequency and time-domain analysis results to substantiate the findings.

## 5. Simulations and results

Simulations are carried out to verify the performance of the proposed ESO based controller in suppression of wing rock motion for time varying angle of attack scenario. The values of the aerodynamic parameters needed in (4) as taken from [23] are

$$c_1=0.354,\qquad c_2=0.001,\qquad g=1.5$$

In simulations, initial conditions for the plant are taken as $x_p(0)=[20^\circ\ 0]$ whereas initial conditions for observer are taken as $\hat{x}(0)=[20^\circ\ 0\ 0]$. The performance specifications are considered in terms of the desired settling time and damping ratio and are taken as $t_s=4$ s and $\zeta=0.8$ and the controller gains, $k_i$s are calculated to meet these requirements. The observer gain, $L$, is obtained by following the pole placement technique by placing the observer error dynamics poles at $[-30,-30,-30]$. The observer and controller are designed at angle of attack $\alpha=21.5^\circ$, i.e., $a_{1o}$ and $a_{2o}$ in (20) and (21) are obtained by using the data corresponding to $\alpha=21.5^\circ$ and are kept the same. The angle of attack variation is effected by using the angle of attack dynamics (5) with command input, $r$, changing between 1 to $-1$ for every 0.5 s. The initial conditions in (5) are taken as $[20^\circ\ 0]^T$. Simulations are carried out and results are presented in Fig. 3. From Fig. 3(a), it can be observed that the controller achieves the task of wing rock motion suppression, i.e., regulating the roll angle to zero quite effectively. Figs. 3(b) and 3(c) show the roll rate and uncertainty estimation respectively and it can be seen that the ESO has estimated the roll

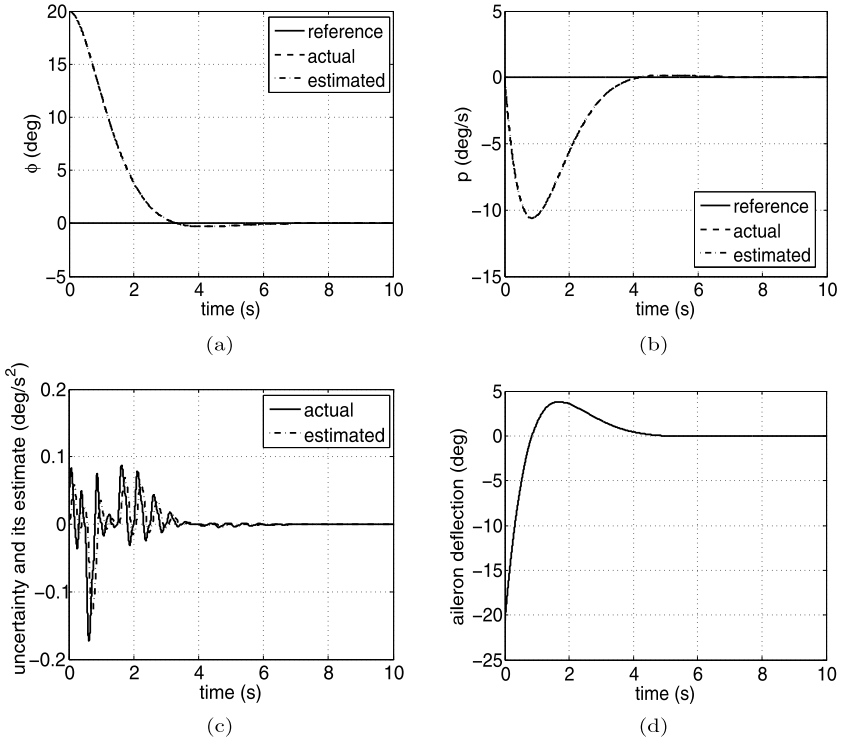


**Fig. 3.** Performance of ESO based controller: State and uncertainty estimation and regulation [$d' = 0$].

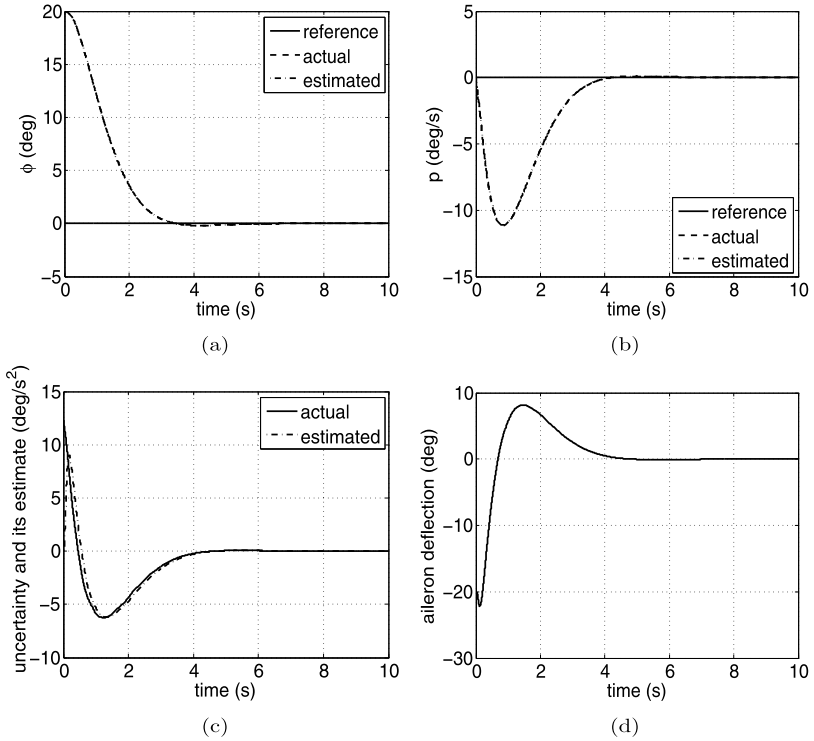


**Fig. 4.** Performance of ESO based controller: State and uncertainty estimation and regulation.

rate as well as the uncertainty quite accurately. Fig. 3(d) shows the control input, i.e., aileron deflection history. To show the effectiveness of the ESO in the presence of external disturbance, it is assumed that an external disturbance, $d'$, as stated in (14) acts on the system. The considered disturbance is [25]

$$d' = 0.6141\phi + 1.2099\dot{\phi} - 0.0513\phi^2\dot{\phi} + 0.035\phi\dot{\phi}^2 + 0.0135\dot{\phi}^3 \tag{32}$$

and the simulation results are presented in Fig. 4. From the figures, it can be observed that the controller achieves the task of wing rock motion suppression quite effectively. It can also be seen that the ESO has estimated the uncertainty and disturbance quite accurately. Next, to show that the controller, with appropriate modification, offers satisfactory performance in tracking a desired roll angle command while suppressing the wing rock motion, simula-

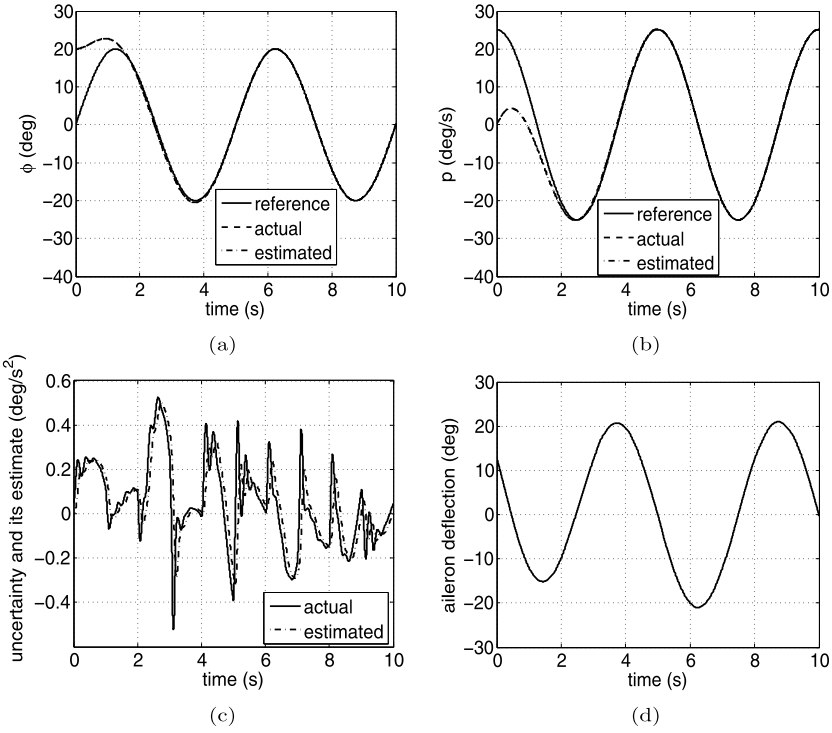


**Fig. 5.** Performance of ESO based controller: State and uncertainty estimation and tracking [$d' = 0$].

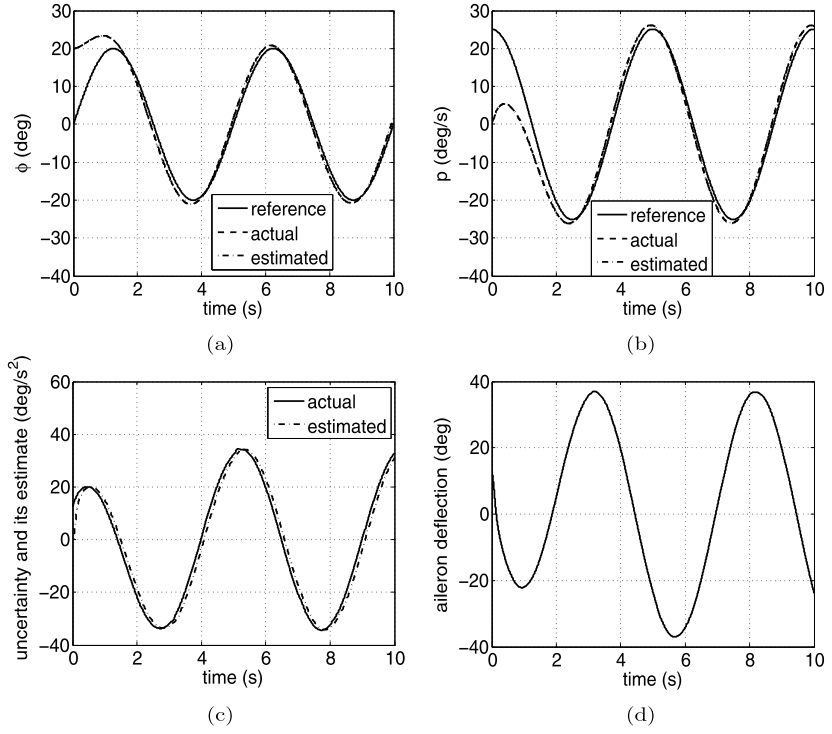


**Fig. 6.** Performance of ESO based controller: State and uncertainty estimation and tracking.

tions are carried out by considering a reference roll angle trajectory as [35]

$$\phi^{\star}(t) = 20\sin(0.4\pi t)\ \text{deg}$$

and the results are presented in Figs. 5 and 6. In Fig. 5, the external disturbance $d'$ is assumed to be zero while the results corresponding to presence of external disturbance are given in Fig. 6. From the figures, it can be observed that the controller offers satisfactory tracking while suppressing the wing rock motion. The profiles of the actual and estimated uncertainty are presented in Figs. 5(c) and 6(c) for the respective case while the corresponding control input histories are given in Figs. 5(d) and 6(d) respectively.

## 6. Comparison with some existing designs

Next, simulations are carried out to compare the performance of the proposed design with some well-known existing con-

**Table 3**
Controller gain values of various design.

| Design | $k_1$ | $k_2$ | $m$ |
|---|---|---|---|
| FL + LQR | 3.1533 | 10.1918 | – |
| Back-stepping | 1.5625 | 2 | – |
| SMC | – | – | 34 |
| ESO based | 1.5625 | 2 | – |

trollers. The controllers considered for the comparison purpose are (a) Feedback Linearization and LQR based design, (b) Back-stepping based control, (c) Variable Structure Control and (d) the proposed ESO based Control. All the controllers are designed at $\alpha = 21.5°$, i.e., the aerodynamic coefficients corresponding to 21.5° have been used in all the designs to ensure that the comparison is valid. A brief of each of the controller is given here for the sake of completeness and the reader may refer to the relevant reference for more details.

*Design-1: Feedback linearization and LQR based design*

In [15], the authors have presented the Feedback Linearization and LQR based design wherein the dynamics is first linearized by following the feedback linearization approach followed by a design of LQR controller for the linearized dynamics. The design is termed as Design-1 in this comparison. The controller for the wing rock dynamics of (4) evaluated at $\alpha = 21.5°$ is given as

$$\delta_{FL+LQR} = -\frac{1}{g}\left(b_1\dot{\phi}^3 + \mu_2\phi^2\dot{\phi} + b_2\phi\dot{\phi}^2\right) - k_1\phi - k_2\dot{\phi} \tag{33}$$

where the controller gains, $k_i$s, are obtained by using the LQR theory wherein the weights, as taken in [15], are $Q = [10\ 0; 0\ 100]$ and $R = 1$.

*Design-2: Back-stepping based control*

A state feedback regulator based on back-stepping algorithm is proposed in [15]. For the wing rock dynamics with time varying angle of attack given by (4), the required back-stepping control law by following the design procedure in [15] is

$$\begin{aligned}\delta_{BS} = &-\frac{1}{g}\left((1 + k_1k_2)\phi + (k_1 + k_2)\dot{\phi}\right)\\ &-\frac{1}{g}\left(-\omega^2\phi + \mu_1\dot{\phi} + b_1\dot{\phi}^3 + \mu_2\phi^2\dot{\phi} + b_2\phi\dot{\phi}^2\right)\end{aligned} \tag{34}$$

The controller gains, $k_i$s, are chosen to satisfy the same performance specifications, i.e., settling time $t_s = 4$ s and damping coefficient $\zeta = 0.8$. The design is referred to as Design-2.

*Design-3: Variable structure control*

A Variable Structure Control (VSC) theory based design presented in [5] is used to derive a control law for the wing rock dynamics of (4). The VSC based control law is

$$\begin{aligned}\delta_{VSC} = &-\frac{1}{g}\left(-\omega^2\phi + \mu_1\dot{\phi} + b_1\dot{\phi}^3 + \mu_2\phi^2\dot{\phi} + b_2\phi\dot{\phi}^2\right)\\ &+\frac{1}{g}\left\{\ddot{r} - m(\dot{\phi} - \dot{r}) - \eta\,\mathrm{sat}\left[\frac{(\dot{\phi} - \dot{r}) + m(\phi - r)}{\rho}\right]\right\}\end{aligned} \tag{35}$$

To meet the performance specifications, controller parameters $r = 0$, $\eta = 3$, $\rho = 0.1$ and $m = 34$ are used. The design is considered as Design-3 for the comparison purpose.

*Design-4: ESO based control*

The proposed ESO based controller given by (21) is designated as Design-4 for the purpose of comparison. Simulation parameters and other design parameters are same as given in Section 5. The values of the controller gains used in the designs are shown in Table 3.

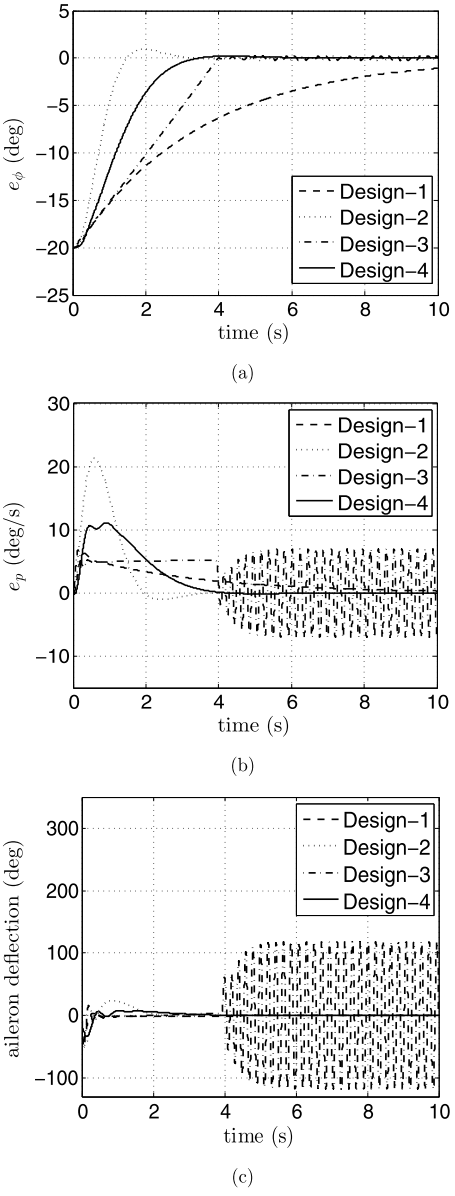


**Fig. 7.** Performance comparison with existing designs.

To compare the performance, simulations are carried out using the data given in Table 1 for all the designs. As stated earlier, the controllers are designed with system coefficients at an angle of attack of 21.5°. A first order actuator dynamics with time constant of 1/15 seconds [23] is considered to bring in the effect of un-modeled dynamics. Further, uncertainty of +10% is introduced in the input gain, $g$, of the system. Lastly, it is assumed that external disturbance, $d'$, of (32) also acts on the system. Other simulation data is kept the same as given in Section 5 and the results are presented in Fig. 7. From Fig. 7(a), it can be seen that while the Designs-1 and -3 have resulted in steady state error in roll regulation, the ESO has offered better wing rock suppression performance. From Figs. 7(b) and (c), it can be observed that Design-3 has severe oscillations in roll rate and aileron deflection. Although the performance of the Design-2 is better in wing rock suppression, it requires large initial control of approximately −60°.

## 7. Performance in presence of sideslip dynamics

Lastly, the performance of the proposed ESO based controller is assessed in the presence of the servo and slide slip dynamics. To

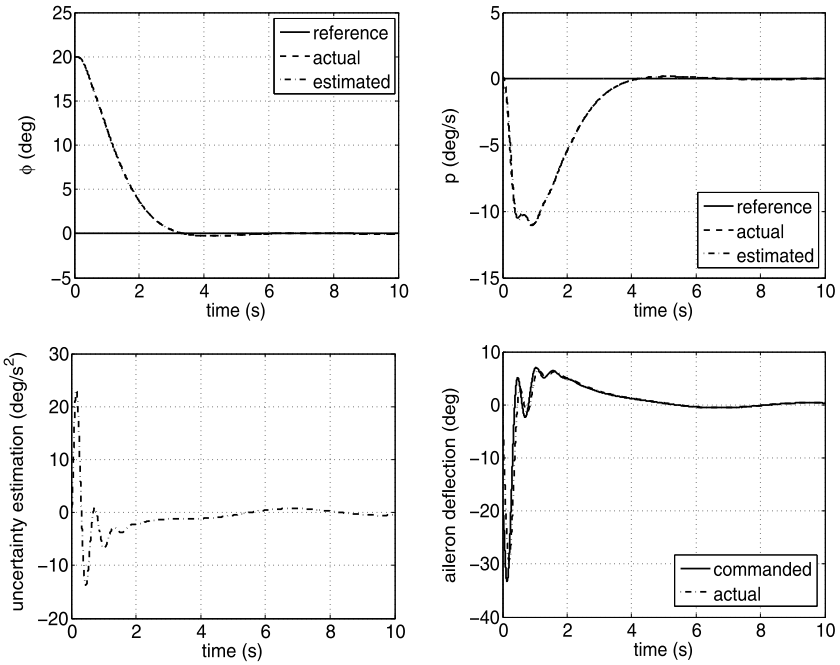


**Fig. 8.** Performance of ESO based controller in presence of un-modeled dynamics: State and uncertainty estimation and regulation.

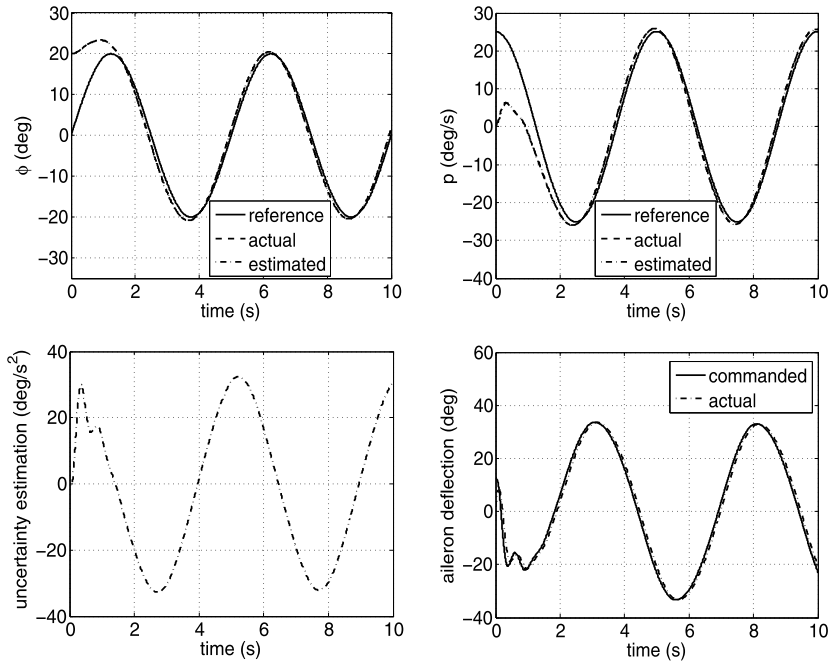


**Fig. 9.** Performance of ESO based controller in presence of un-modeled dynamics: State and uncertainty estimation and tracking.

this end, consider a wing rock model [36,45] that includes servo as well as sideslip dynamics

$$\begin{aligned}
\dot{x}_1 &= x_2\\
\dot{x}_2 &= -\omega^2 x_1 + \mu_1 x_2 + b_1 x_2^3 + \mu_2 x_1^2 x_2 + b_2 x_1 x_2^2 + L_\beta x_4\\
&\quad - L_r x_5 + L_\delta x_3\\
\dot{x}_3 &= -\frac{1}{\tau} x_3 + \frac{1}{\tau}\delta_c\\
\dot{x}_4 &= x_5\\
\dot{x}_5 &= -N_p x_2 - N_\beta x_4 + N_r x_5\\
y &= x_1
\end{aligned} \tag{36}$$

where $x = [x_1\ x_2\ x_3\ x_4\ x_5]^T = [\phi\ \dot{\phi}\ \delta\ \beta\ \dot{\beta}]^T$. The state variables $\phi$, $\dot{\phi}$, $\delta$, $\beta$ and $\dot{\beta}$ represent the roll angle, roll rate, aileron deflection, sideslip angle and sideslip angle rate respectively whereas $\delta_c$ is the commanded aileron deflection. The quantities $L_\beta$, $L_\delta$, $L_r$ $N_p$, $N_\beta$ and $N_r$ are the aerodynamics moment derivatives not considered in the wing rock roll dynamics of (4). It may be noted that the dynamics (36) contains a first order servo dynamics with a time constant of $\tau$. As the sideslip related aerodynamic data needed in (36) is available only for an angle of attack of 25° in [45], the aerodynamic quantities corresponding to the fixed angle of attack of 25° only are used in the simulations.

To investigate performance in the presence of servo and sideslip dynamics, simulations are carried out using the proposed ESO

based controller for the wing rock model of (36). It may be noted that the ESO based controller is designed at an angle of attack of 21.5° for the roll dynamics of (4) and therefore, the servo and sideslip dynamics present in (36) represent un-modeled dynamics for the controller. In plant, the data corresponding to $\alpha = 25°$ as given in [45] is used. Plant initial conditions are taken as $x_p(0) = [20\ 0\ 0\ 10\ 0]°$, whereas initial conditions for observer are taken as $\hat{x} = [20°\ 0\ 0]$. Further, it is assumed that an external disturbance, $d'$, as given in (32) and uncertainty of +10% is present in the input gain, $g$. Simulations are carried out and the results are presented in Fig. 8. From Fig. 8(a), it can be observed that the controller achieves the task of wing rock motion suppression, i.e., regulating the roll angle to zero quite effectively. Figs. 8(b) and 8(c) show the roll rate and uncertainty estimation respectively whereas the corresponding aileron deflection histories, i.e., commanded and actual aileron deflection histories are given in Fig. 8(d). As the controller designed for the roll dynamics is employed for the 5th order dynamics of (36), the actual uncertainty could not be computed and therefore, only the estimated uncertainty is given in Fig. 8(c).

Next, to show that the controller, with appropriate modification, offers satisfactory performance in tracking a desired time-varying roll angle command while suppressing the wing rock motion, simulations are carried out by considering a reference roll angle trajectory as $\phi^\star(t) = 20\sin(0.4\pi t)$ deg and the results are presented in Fig. 9. From the figures, it can be observed that the controller has offered satisfactory tracking while suppressing the wing rock motion. The profiles of estimated uncertainty is presented in Fig. 9(c) whereas the corresponding control input histories are given in Fig. 9(d). From the simulation results, it becomes obvious that the proposed ESO based controller has offered satisfactory performance in the presence of the un-modeled dynamics of sideslip.

## 8. Conclusion

In this paper an ESO based controller is proposed for the design of a wing rock suppression. System states and the effect of uncertainties are estimated by ESO in an integrated manner. An IOL controller is augmented by the estimated disturbance to cancel its effect. Simulation results show that the proposed design is robust and offers satisfactory performance in presence of uncertainties, external disturbances as well as un-modeled dynamics. Performance comparison of the proposed design with some well-known controllers shows that the proposed design offers better performance.

## References


[1] E.N. Abdulwahab, C. Hongquan, Periodic motion suppression based on control of wing rock in aircraft lateral dynamics, Aerosp. Sci. Technol. 12 (2008) 295–301.

[2] A.D. Araujo, S.N. Singh, Variable structure adaptive control of wing-rock motion of slender delta wings, J. Guid. Control Dyn. 21 (2) (1998) 251–256.

[3] E. Capello, G. Guglieri, D. Sartori, Performance evaluation of an $L_1$ adaptive controller for wing-body rock suppression, J. Guid. Control Dyn. 35 (6) (2012) 1702–1708.

[4] W.-H. Chen, Nonlinear disturbance observer-enhanced dynamic inversion control of missile, J. Guid. Control Dyn. 26 (1) (2003) 161–166.

[5] J.L. Crassidis, Robust control of nonlinear systems using model error control synthesis, J. Guid. Control Dyn. 22 (4) (1999) 595–601.

[6] J.M. Elzebda, A.H. Nayfeh, D.T. Mook, Development of an analytical model of wing rock for slender delta wings, J. Aircr. 26 (8) (1989) 737–743.

[7] G. Feng, Y.-F. Liu, L. Huang, A new robust algorithm to improve the dynamic performance on the speed control of induction motor drive, IEEE Trans. Ind. Electron. 19 (6) (2004) 1614–1627.

[8] Z. Gao, Scaling and bandwidth-parametrization based controller tuning, in: Proc. of the American Control Conference, Denver, Colorado, USA, 2003, pp. 4989–4996.

[9] Z. Gao, Y. Huang, J. Han, An alternative paradigm for control system design, in: Proc. of the 40th IEEE Conference on Decision and Control, Orlando, Florida, USA, 2001, pp. 4578–4585.

[10] A.A. Godbole, J.P. Kolhe, S.E. Talole, Performance analysis of generalized ESO in tackling sinusoidal disturbances, IEEE Trans. Control Syst. Technol. 21 (6) (2013) 2212–2223.

[11] G. Guglieri, F. Quagliotti, Experimental observation and discussions of the wing rock phenomenon, Aerosp. Sci. Technol. 2 (1997) 111–123.

[12] C.E. Hall, Y.B. Shtessel, Sliding mode disturbance observer-based control for a reusable launch vehicle, J. Guid. Control Dyn. 29 (6) (2006) 1315–1328.

[13] J. Han, From PID to active disturbance rejection control, IEEE Trans. Ind. Electron. 56 (3) (2009) 900–906.

[14] C.-H. Hsu, C.E. Lan, Theory of wing rock, J. Aircr. 22 (10) (1985) 920–924.

[15] G. Jee, S.K. Zachariah, M.V. Dhekane, B.B. Das, Comparison of LQR, feedback linearization and back stepping based control laws for suppressing wing rock, in: Proceedings of the International Conference on Aerospace Science and Technology, Bangalore, India, 2008, pp. 1–5.

[16] W. Kim, C.C. Chung, Robust high order augmented observer based control for nonlinear systems, in: Proceedings of the IEEE Conference on Decision and Control, Maui, Hawaii, USA, 2012, pp. 919–924.

[17] Z.L. Liu, C.-Y. Su, J. Svoboda, Variable phase control of wing rock, Aerosp. Sci. Technol. 10 (2006) 27–35.

[18] Z.L. Liu, J. Svoboda, A new control scheme for nonlinear systems with disturbances, IEEE Trans. Control Syst. Technol. 14 (1) (2006) 176–181.

[19] J. Luo, C.E. Lan, Control of wing-rock motion of slender delta wings, J. Guid. Control Dyn. 16 (2) (1993) 225–231.

[20] M.M. Monahemi, M. Krstic, Control of wing rock motion using adaptive feedback linearization, J. Guid. Control Dyn. 19 (4) (1996) 905–912.

[21] J.T. Moura, H. Elmali, N. Olgac, Sliding mode control with sliding perturbation observer, Trans. ASME, J. Dyn. Syst. Meas. Control 119 (4) (1997) 657–665.

[22] A.H. Nayfeh, J.M. Elzebda, D.T. Mook, Analytical study of the subsonic wing-rock phenomenon for slender delta wings, J. Aircr. 26 (9) (1989) 805–809.

[23] R. Ordonez, K.M. Passino, Wing rock regulation with a time-varying angle of attack, in: Proceedings of the 15th IEEE International Symposium on Intelligent Control (ISIC 2000), Rio, Patras, Greece, 2000, pp. 145–150.

[24] K.S. Priyamvada, V. Olikal, S.E. Talole, S.B. Phadke, Robust height control system design for sea skimming missiles, J. Guid. Control Dyn. 34 (6) (2011) 1746–1756.

[25] S.-P. Shue, R.K. Agarwal, Nonlinear $H_\infty$ method for control of wing rock motions, J. Guid. Control Dyn. 23 (1) (2000) 60–68.

[26] S.-P. Shue, M.E. Sawan, K. Rokhsaz, Optimal feedback control of a nonlinear system: Wing rock example, J. Guid. Control Dyn. 19 (1) (1996) 166–171.

[27] S.N. Singh, W. Yim, W.R. Wells, Direct adaptive and neural control of wing-rock motion of slender delta wings, J. Guid. Control Dyn. 18 (1) (1995) 25–30.

[28] J.-J.E. Slotine, W. Li, Applied Nonlinear Control, Prentice-Hall, Englewood Cliffs, New Jersey, 1991.

[29] Y.X. Su, B.Y. Duan, C.H. Zheng, Y.F. Zhang, G.D. Chen, J.W. Mi, Disturbance-rejection high-precision motion control of a Stewart platform, IEEE Trans. Control Syst. Technol. 12 (3) (2004) 364–374.

[30] J. Su, W. Qiu, H. Ma, P.-Y. Woo, Calibration-free robotic eye–hand coordination based on an auto disturbance rejection controller, IEEE Trans. Robot. 20 (5) (2004) 899–907.

[31] D. Sun, Comments on active disturbance rejection control, IEEE Trans. Ind. Electron. 54 (6) (2007) 3428–3429.

[32] R.H.C. Takahashi, P.L.D. Peres, Unknown input observers for uncertain systems: A unifying approach and enhancements, in: Proceedings of the 35th Conference on Decision and Control, Kobe, Japan, 1996, pp. 1483–1488.

[33] S.E. Talole, A.A. Godbole, J.P. Kolhe, S.B. Phadke, Robust roll autopilot design for tactical missiles, J. Guid. Control Dyn. 34 (1) (2011) 107–117.

[34] S.E. Talole, J.P. Kolhe, S.B. Phadke, Extended-state-observer-based control of flexible-joint system with experimental validation, IEEE Trans. Ind. Electron. 57 (4) (2010) 1411–1419.

[35] S.E. Talole, S.B. Phadke, Robust input–output linearisation using uncertainty and disturbance estimation, Int. J. Control 82 (10) (2009) 1794–1803.

[36] A. Tewari, Modern Control Design with MATLAB and SIMULINK, John Wiley & Sons, Ltd., Chichester, West Sussex, UK, 2002.

[37] W. Wang, Z. Gao, A comparison study of advanced state observer design techniques, in: Proc. of the American Control Conference, Denver, Colorado, USA, 2003, pp. 4754–4759.

[38] Y. Xia, Z. Zhu, M. Fu, Back-stepping sliding mode control for missile systems based on an extended state observer, IET Control Theory Appl. 5 (1) (2011) 93–102.

[39] Y. Xia, Z. Zhu, M. Fu, S. Wang, Attitude tracking of rigid spacecraft with bounded disturbances, IEEE Trans. Ind. Electron. 58 (2) (2011) 647–659.

[40] D. Yoo, S.S.-T. Yau, Z. Gao, Optimal fast tracking observer bandwidth of the linear extended state observer, Int. J. Control 80 (1) (2007) 102–111.

[41] K. Youcef-Toumi, O. Ito, A time delay controller for systems with unknown dynamics, Trans. ASME, J. Dyn. Syst. Meas. Control 112 (1) (1990) 133–142.

[42] R. Zhang, C. Tong, Torsional vibration control of the main drive system of a rolling mill based on an extended state observer and linear quadratic control, J. Vib. Control 12 (3) (2006) 313–327.
[43] Q. Zheng, L. Dong, D.H. Lee, Z. Gao, Active disturbance rejection control for MEMS gyroscopes, IEEE Trans. Control Syst. Technol. 17 (6) (2009) 1432–1438.
[44] Q. Zheng, L.Q. Gao, Z. Gao, On validation of extended state observer through analysis and experimentation, J. Dyn. Syst. Meas. Control 134 (2012) 024505, 1–6.
[45] M. Zribi, S. Alshamali, M. Al-Kendari, Suppression of the wing-rock phenomenon using nonlinear controllers, Nonlinear Dyn. 71 (1–2) (2013) 313–322.